Observation of Polaron Dynamics in Magnetic Quantum Wells

D. D. Awschalom,[1] M. R. Freeman,[1] N. Samarth,[2] H. Luo,[2] and J. K. Furdyna[2]

[1]*IBM Watson Research Center, P.O. Box 218, Yorktown Heights, New York 10598*

[2]*Department of Physics, University of Notre Dame, Notre Dame, Indiana 46556*

Femtosecond spectroscopic measurements of optically induced magnetization are performed on new type-II ZnTe/Cd$_{1-x}$Mn$_x$Se diluted-magnetic-semiconductor heterostructures consisting of magnetic quantum wells confined by nonmagnetic barrier layers. The formation and evolution of electron-based bound magnetic polarons in the wells is observed through static and time-domain experiments. Energy-dependent magnetic spin dynamics on ultrashort time scales are seen to vary dramatically with the degree of electronic confinement.

The very strong spin interactions and good optical properties of magnetic semiconductors enable unique real-time observations of ultrafast spin dynamics in these systems.[1] Time-resolved techniques in concert with a variety of magnetic and optical probes have produced a relatively complete view of the magnetic response to pulsed optical injection of charge carriers of specific spin polarization.[2] Furthermore, crystal growth of ultrathin-layered structures by molecular-beam epitaxy has made it possible to examine the crossover behavior of magnetic effects to lower dimensions.[3] One of the most interesting properties of bulk magnetic semiconductor systems is the tendency to form a cluster of oriented ionic spins within the Bohr radius of a charge carrier, known collectively as a magnetic polaron (MP).[4] Three-dimensional polaron dynamics have been studied through time-resolved measurements of the ionic magnetization, both directly[5] and via the Faraday rotation,[1] and through optical transmission[6] and luminescence[7] experiments. In lower dimensions, polaronic effects should be influenced by compression of the carrier wave functions on the scale of the polaron radius in bulk material, and by the reduction of magnetic layer thicknesses to a quasi-two-dimensional regime. One may therefore exploit the possibility afforded by semiconductor quantum wells to selectively vary the electronic and magnetic degrees of freedom to explore the role of dimensionality in microscopic spin organization.

In this work we present the first magnetic studies of a new class of II-VI diluted-magnetic-semiconductor heterostructures,[8] in which the magnetic material is entirely confined to the lower band-gap quantum-well regions. These structures have a type-II band alignment, with the holes spatially separated from the magnetic layers, leaving a clean experimental situation in which electrons alone interact with the magnetic ions in a well-defined geometry and for which effects arising through electron-hole exchange may be neglected. The length scales are such that the electronic wave functions may be significantly compressed along the normal to the planes, creating a two-dimensional environment for the electronic de-grees of freedom, while the magnetic ions continue to interact as in bulk, apart from an effective dilution as the surface-to-volume ratio of the layers increases. This allows the exploration of the dimensional dependence of magnetic polaron behavior, in particular for donor-bound MP, the simplest type of polaron. Optically generated, spin-aligned carriers induce a magnetization which in the present experiments is detected by a sensitive susceptometer. Strikingly, polarons are clearly observed even for well widths as narrow as one-third the polaron diameter in the corresponding bulk material, with the in-plane diameter nearly unchanged. We observe an increase in the MP formation and decay times toward lower well dimensions consistent with an effectively lower magnetic concentration seen by the electrons. Moreover, measurements on ultrafast time scales (~ 150 fs) reveal clear evidence of an additional fast time constant owing to carrier-ion spin scattering.

Multiple-quantum-well samples of Cd$_{1-x}$Mn$_x$Se confined by ZnTe barriers are grown by molecular-beam epitaxy (MBE) upon 2-μm-thick ZnTe buffer layers on (100) GaAs substrates. Sample growth is monitored *in situ* by 10-keV reflection high-energy electron diffraction. The post growth characterization of ZnTe/Cd$_{1-x}$Mn$_x$Se heterostructures and superlattices by transmission electron microscopy (TEM), x-ray diffraction, and optical measurements will be reported elsewhere.[8] MBE-grown Cd$_{1-x}$Mn$_x$Se stabilizes in the cubic zinc-blende phase, while bulk-growth techniques result in the hexagonal wurtzite phase.[9] Optical-absorption and -reflection spectra and the absence of excitonic luminescence indicate a type-II band alignment in ZnTe/Cd$_{1-x}$Mn$_x$Se, with electrons confined to the Cd$_{1-x}$Mn$_x$Se layers and holes in the ZnTe layers.[8] Samples constituting a series of well widths (28, 56, and 84 Å) confined by fixed-width (160 Å) barriers are studied in the present work for two different magnetic concentrations ($x = 0.13, 0.23$).

An integrated dc SQUID microsusceptometer[10] forms the core of the apparatus for direct measurements of optically induced magnetization. For dynamical studies,

the time dependence of this magnetization is recorded by a pump–time-delayed-probe technique taking advantage of the nonlinear magneto-optical susceptibility of the Mn^{2+} sublattice.[11] The present magnetometer, top loaded in an optical cryostat, offers direct access to the samples through transparent windows. The avoidance of an optical fiber and its inherent frequency dispersion allows true femtosecond time resolution to be achieved. The samples are excited by fiber-prism compressed circularly polarized optical pulses 150 fs in duration from a two-jet dye laser synchronously pumped by a frequency-doubled mode-locked Nd-doped yttrium aluminum garnet source, thereby instantaneously creating spin-polarized carriers. A superconducting shield surrounds the magnetometer and maintains an effectively zero-field environment of $\sim 10^{-2}$ mT. For the measurements presented here the sample and SQUID are immersed in superfluid ^{4}He at 1.5 K. The coupled energy sensitivity of the SQUID system corresponds to an ability to detect $\sim 10^4$ aligned ionic spins.

The first indication of polaron formation in these structures comes from the data of Fig. 1. Here the time-averaged magnetization induced by circularly polarized light is shown for the $x = 0.23$ series of structures as a function of excitation energy in the vicinity of the quantum-well ground-state level, yielding a *magnetic* excitation spectrum analogous to more familiar photoluminescence excitation spectra. A well-defined peak due to magnetic polarons is observed in each case, in-

cluding the wells which are narrow in comparison to the estimated polaron diameter (90 Å) in bulk. With increasing photon energy, the magnetization first increases sharply with the onset of absorption from the radiation field into impurity levels at which polarons may form. The states most favorable for polaron formation are at donor sites with a local magnetic environment, determined by the statistically random arrangement of Mn^{2+} spins in zero applied field, such that a magnetic free-energy minimum already exists along the axis defined by the incident photon angular momentum. Thus the polarons formed have a well-defined orientation and contribute a net magnetic signal. For higher photon energies, memory of the initial carrier orientation is lost to a large degree through spin scattering during the energy relaxation process. The polarons which subsequently form are randomly oriented and do not contribute to the magnetic signal. This causes a decrease in the optically induced magnetization, leaving a striking resonancelike peak for each sample at an energy which varies in the range from 10 to 25 meV below the lowest excitonic energy level ($n = 1$) in the well as determined by photoreflectance (and indicated by the arrows in the figure). The ground-state level shifts to higher energies with increasing confinement as predicted by simple Kronig-Penney-type models.

The energy shift of the polaron with respect to the $n = 1$ level is determined by the sum of two contributions, a dominant electrostatic piece which is the binding energy of the electron at a donor, and a far smaller magnetic (exchange) piece from the binding energy of the polaron itself. As seen in Fig. 1, the energy shift has a maximum at intermediate well widths, in agreement with the trend found for quantum-confined hydrogenic donors;[12] although quantitative comparisons require the knowledge of many unknown parameters such as the positions of the impurities within the well, the overall energy scale is consistent with this expectation. Polaron binding energies as a function of confinement are also expected first to increase as the electronic wave function becomes compressed, and subsequently to decrease as the effective magnetic concentration seen by the carriers diminishes when the confining planes become very thin. However, shifts of more than 1 meV occur only for complexes involving holes, in particular excitons bound to neutral acceptors. The absence of a noticeable temperature dependence of the energy shift at low temperatures also lends support to the contention that it is largely electrostatic in origin.

The dynamical aspects of the optically induced magnetization may be studied using a stroboscopic scheme which exploits the nonlinear response of the magnetic sublattice,[11] where one observes the component of magnetization transferred to the Mn^{2+} ions from the initially spin-polarized optically excited carriers by spin-flip scattering. Figure 2 illustrates the time dependence of the magnetization induced by subpicosecond optical
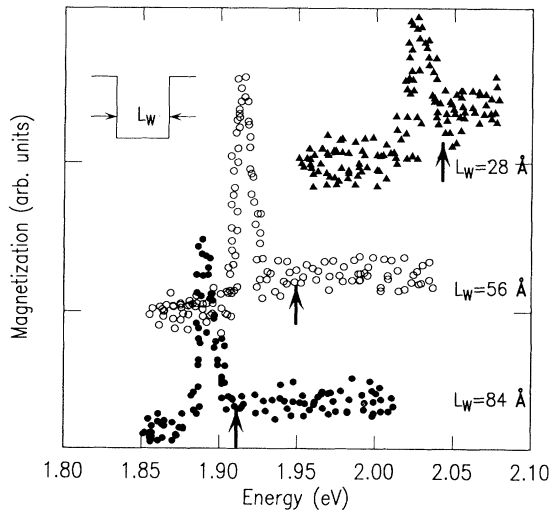

FIG. 1. Magnetic excitation spectra of three multiple-quantum-well heterostructures having well widths of 28, 56, and 84 Å, and ZnTe barrier thicknesses of 160 Å. The resonancelike peaks are the signatures of magnetic polaron formation, while the energy gaps as determined by reflectance spectroscopy are indicated by the arrows. The y tick marks indicate the relative zeros of magnetization. $T = 1.5$ K, power $= 100$ μW, number of periods $= 30$, 15, and 10, respectively.
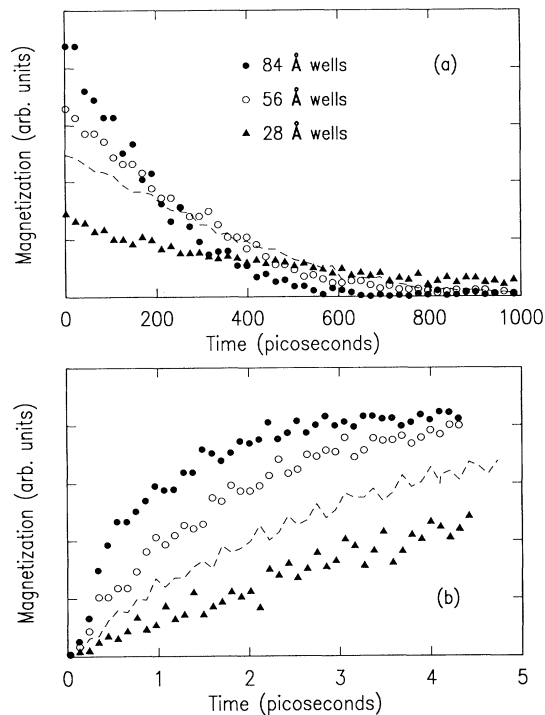
FIG. 2. Time dependence of the optically induced magnetization as determined by time-resolved magnetic spectroscopy for above-band-gap excitation energies. (a) Spin-lattice relaxation of the magnetization; the solid circles, open circles, and solid triangles, respectively, represent the 84-, 56-, and 28-Å well samples of Fig. 1, while the dashed line is a measurement of an 84-Å, 13% Mn well structure. (b) Initial rise of the magnetization in response to excitation pulse of 150-fs duration.

pulses as a function of quantum-well width and magnetic concentration, for excitation energies in the plateau regions above the polaron peaks seen in the static spectra of Fig. 1. Figure 2(a) shows the spin-lattice relaxation of the magnetization. These signals evolve long after the electronic spins have depolarized. The curves represented by symbols show a significant dependence of relaxation rate on well thickness when the Mn concentration is held at a fixed value (here 23%). The magnetic environment experienced by the ions is therefore changing with the layer thickness. This effect can be described phenomenologically in terms of a decrease in the effective magnetic concentration with decreasing thickness, owing to the fact that Mn atoms next to the interfaces see fewer magnetic neighbors. A comparison between wide well samples having different Mn concentration [the solid circles and dashed line in Fig. 2(a)] suggests that the actual dependence of the relaxation rate on concentration is approximately linear in this regime. This concentration dependence indicates that some form of cross relaxation involving pairs or larger clusters of ions is taking place, with our observations likely in the saturation regime of a stronger power law at small x.

The femtosecond resolution enabled by the direct optical access of the present apparatus also allows the *onset* of the time-dependent optically induced magnetization to be inspected with great clarity, as shown in Fig. 2(b). The rate at which this magnetization grows to its saturation value is determined by the strength of spin-flip scattering with the optically excited carriers (we emphasize that this measurement does not record the magnetization of the carriers themselves). Although this growth can be limited by the spin-lattice relaxation of carriers via other mechanisms, in the present situation the electron-ion mechanism should dominate both because of the high Mn concentration and because exchange effects on the electrons are minimized by the real-space separation of electrons and holes. The picosecond-scale times are consistent with spin-flip times calculated and measured for other semimagnetic II-VI systems.[13,14] Direct magnetic measurements provide a unique means of probing this interaction for type-II heterostructures. The magnetization onset times follow the same trend as a function of well dimension as the decay times from Fig. 2(a), although the concentration dependence deduced from the comparison of different wide wells is slightly stronger here. This is somewhat surprising given that the electronic spin-flip rates should be proportional to the number of unpaired Mn^{2+} ions, a quantity that saturates sharply at small x due to the large number of nearest-neighbor sites. The effective magnetic concentration factors into the variation of time scales here, as in the ionic spin-lattice relaxation. The electronic degrees of freedom also influence the rate and can change with the well dimension, although in the present measurements the carriers are always excited into the lowest subband.

Polaron formation dramatically alters the dynamical behavior of the magnetization, as found in the curves plotted in Fig. 3 for excitations at the polaron energies. The growth of the magnetization over a time scale of hundreds of picoseconds is a result of relaxation of Mn^{2+} ions to produce spin-aligned clusters around donor sites, a net magnetization arising because of the initial optically induced orientation of the carriers. We therefore observe in the time domain the origin of the strong peak of the magnetization found in the static spectra (Fig. 1). The polaronic magnetization ultimately decays according to the dynamics of this localized spin complex. An additional component of the magnetization from spin-flip scattering with some carriers appears as a knee in the very-short-time response [Fig. 3(b)].

It is again remarkable in Fig. 3 that the polaron signature is so apparent even for the narrowest wells. The various curves have been normalized to account for different total quantities of magnetic material in each sample, such that the absolute amplitude of the different signals may be directly compared. From the dynamical data we are able to estimate how the polaron shape evolves with increasing confinement, subject to the as-
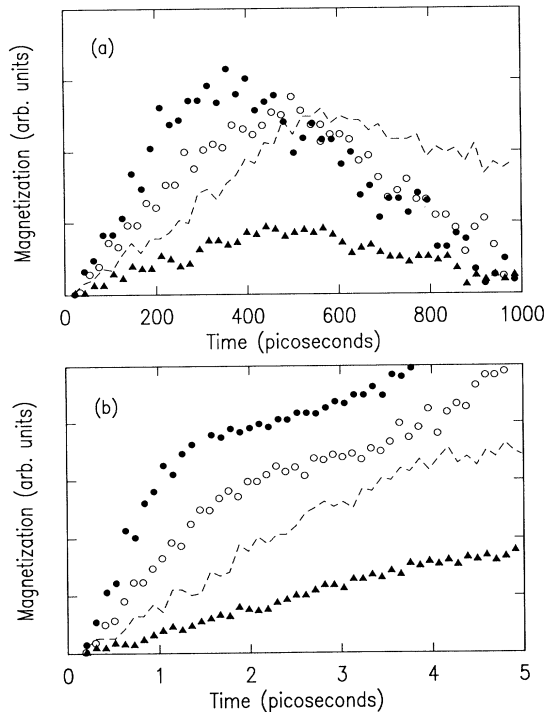
FIG. 3. Time-dependent magnetization for the samples of Fig. 2 with pulsed excitation at the peak polaron energies determined from static spectra as in Fig. 1. (a) Long-time scan showing the polaronic life cycle. (b) Short-time scan showing the additional time constant due to electron-ion spin-flip scattering.

sumption that the probability per photon absorbed of forming an oriented polaron is a constant for all samples. With the growth and decay of the polaron magnetization governed by the spin-lattice time, deduced from Fig. 2(a), it is straightforward to estimate the peak magnetization that would occur if the polarons were allowed to evolve to completion (not limited by the carrier lifetime). By this procedure we find that the in-plane polaron diameter remains, within the accuracy of the data, roughly constant at the bulk value of ~90 Å, independent of the well width. Moreover, this interpretation is consistent with an analysis of the dc spectra of Fig. 1 using the measured spin-lattice times as additional input. The increased spin-lattice time for narrower wells explains how the peak height of the polaron magnetization evolves relative to the plateau at higher energies in the dc spectra of Fig. 1. For the high-energy plateaus, given an initial magnetization, the time-integrated value increases in proportion to the spin-lattice time. However, in the case of a polaron, if we assume the growth and decay to be governed by the spin-lattice time, the integrated magnetization depends only on the carrier spin lifetime. The dc peak heights therefore reflect either the number of pola-

rons created or, we assume, the number of spins per polaron, allowing us to again estimate the polaron diameter.[15]

In summary, femtosecond measurements of optically induced magnetization in new II-VI magnetic heterostructures incorporating genuine magnetic quantum wells reveal a rich variety of energy-dependent spin behavior. Direct evidence of bound magnetic polaron formation is observed in quantum structures even for layer thicknesses small compared to the three-dimensional polaron diameter. The data indicate that the in-plane polaron diameter remains roughly constant at the three-dimensional value, independent of the well width. A real-time view of picosecond electron-ion spin-flip scattering in these structures is also obtained, from the measurement of the onset of optically induced magnetization with femtosecond time resolution.

[1]D. D. Awschalom et al., Phys. Rev. Lett. 55, 1128 (1985).

[2]D. D. Awschalom and M. R. Freeman, in Localization and Confinement of Electrons in Semiconductors, edited by K. von Klitzing (Springer-Verlag, New York, 1990).

[3]J. M. Hong et al., J. Appl. Phys. 63, 3285 (1988).

[4]T. Kasuya and A. Yanase, Rev. Mod. Phys. 40, 684 (1968).

[5]D. D. Awschalom, J. Warnock, and S. von Molnar, Phys. Rev. Lett. 58, 812 (1987).

[6]J. H. Harris and A. V. Nurmikko, Phys. Rev. Lett. 51, 1472 (1983).

[7]W. Hayes et al., J. Lumin. 40, 72 (1988).

[8]N. Samarth, H. Luo, J. Buschert, J. K. Furdyna, K. Mahalingam, N. Otsuka, W. Chou, and A. Petrou (to be published).

[9]N. Samarth, H. Luo, J. K. Furdyna, S. B. Qadri, Y. R. Lee, A. K. Ramdas, and N. Otsuka, J. Electron. Mater. 19, 543 (1990).

[10]D. D. Awschalom et al., Appl. Phys. Lett. 53, 2108 (1988).

[11]J. Warnock and D. D. Awschalom, Jpn. J. Appl. Phys. 26, 819 (1987).

[12]G. Bastard, Wave Mechanics Applied to Semiconductor Heterostructures (Les Editions de Physique, Paris, 1988), pp. 125 and 126. We note that although the CdMnSe layers are not intentionally doped, there is a tendency for as-grown CdMnSe to be n type.

[13]G. Bastard and L. L. Chang, Phys. Rev. B 41, 7899 (1990).

[14]M. R. Freeman et al., J. Appl. Phys. 67, 5102 (1990).

[15]The numbers obtained agree with the other estimate at the 50% level. In general, many other factors should be taken into consideration, such as a difference in growth and decay rates since a carrier is present in one case and absent in the other, and the effective magnetic concentration relating the number of spins in the polaron to its actual size.